Structural phase transitions and fundamental band gaps of $Mg_xZn_{1-x}O$ alloys from first principles

I. V. Maznichenko,[1] A. Ernst,[2,3,*] M. Bouhassoune,[2,4] J. Henk,[2] M. Däne,[1,5] M. Lüders,[6] P. Bruno,[2,7] W. Hergert,[1] I. Mertig,[1,2] Z. Szotek,[6] and W. M. Temmerman[6]

[1]*Institut für Physik, Martin-Luther-Universität Halle-Wittenberg, D-06099 Halle, Germany*

[2]*Max-Planck-Institut für Mikrostrukturphysik, Weinberg 2, D-06120 Halle, Germany*

[3]*Donostia International Physics Center (DIPC), Paseo de Manuel Lardizabal 4, 20018 San Sebastián/Donostia, Basque Country, Spain*

[4]*Department Physik, Universität Paderborn, 33095 Paderborn, Germany*

[5]*Materials Science and Technology Division, Oak Ridge National Laboratory, Oak Ridge, Tennessee 37831, USA*

[6]*Daresbury Laboratory, Daresbury, Warrington WA4 4AD, United Kingdom*

[7]*European Synchrotron Radiation Facility, BP 220, F-38043 Grenoble Cedex, France*

(Received 29 April 2009; revised manuscript received 27 June 2009; published 6 October 2009)

The structural phase transitions and the fundamental band gaps of $Mg_xZn_{1-x}O$ alloys are investigated by detailed first-principles calculations in the entire range of Mg concentrations x, applying a multiple-scattering theoretical approach (Korringa-Kohn-Rostoker method). Disordered alloys are treated within the coherent-potential approximation. The calculations for various crystal phases have given rise to a phase diagram in good agreement with experiments and other theoretical approaches. The phase transition from the wurtzite to the rock-salt structure is predicted at the Mg concentration of $x=0.33$, which is close to the experimental value of 0.33–0.40. The size of the fundamental band gap, typically underestimated by the local-density approximation, is considerably improved by the self-interaction correction. The increase in the gap upon alloying ZnO with Mg corroborates experimental trends. Our findings are relevant for applications in optical, electrical, and, in particular, in magnetoelectric devices.

DOI: 10.1103/PhysRevB.80.144101 PACS number(s): 61.50.Ks, 81.30.Hd

I. INTRODUCTION

In recent years, much effort has been devoted to research on ZnO, inspired mostly by its attractive properties for optoelectronic applications.[1] This interest arises from specific properties, e.g., a large piezoelectric coefficient, photoconductivity, and transparency in the visible and infrared wavelength regimes. The range of applications of this semiconductor can be considerably extended by alloying. Prominent dopants are Co and, in particular, Mg, on which we focus in this work. An increase in the Mg concentration can transform the crystal lattice from the wurtzite (WZ) structure of ZnO to the rock-salt (RS) structure of MgO. Accompanied by this structural phase transition is a substantial increase in the fundamental band gap. The latter can be tuned from 3.35 to 7.7 eV.[1,2] In view of a possible band-gap engineering, $Mg_xZn_{1-x}O$ alloys may also be considered as suitable insulating spacers in magnetoelectronic devices, in particular, in magnetic tunnel junctions.

According to the equilibrium phase diagram,[3,4] the solid solution of $Mg_xZn_{1-x}O$ is of eutectic type at normal conditions. It is characterized by an extensive solubility of zincite in MgO (up to 33 mol %) and by a restricted solubility of MgO in ZnO (4 mol %). The solubility depends strongly on experimental conditions and can be considerably increased at high temperatures and high pressures.[5,6] Nonequilibrium growth processes, such as pulsed laser deposition (PLD) (Refs. 7–11) and molecular-beam epitaxial methods,[12–15] allow to grow high-quality $Mg_xZn_{1-x}O$ thin films for a large range of concentrations x. For **RS**-$Mg_xZn_{1-x}O$, produced by PLD, a maximum solubility has been reported for $x=0.5$.[9,16] When increasing the Zn concentration, the RS and the WZ phases separate, and $Mg_xZn_{1-x}O$ exhibits a WZ structure for $x<0.4$.[17] The solubility limit and the phase formation in $Mg_xZn_{1-x}O$ are strongly influenced by experimental conditions and by the substrate on which the $Mg_xZn_{1-x}O$ film is grown. In general, alloying of ZnO and MgO proceeds by substituting Mg atoms by Zn atoms in the cubic RS structure and *vice versa* in the hexagonal WZ structure.

The composition and the crystalline structure affect directly the electronic properties of $Mg_xZn_{1-x}O$. Numerous absorption and photoluminescence spectroscopy experiments show that the fundamental band gap depends differently on the Zn concentration in the RS and WZ phases.[18,19] The width of the band gap increases almost linearly with Mg concentration for both the RS and the WZ phase but the slope in cubic $Mg_xZn_{1-x}O$ is about twice as large as in the hexagonal structure.[20] This experimental finding clearly indicates that $Mg_xZn_{1-x}O$ is a promising candidate for band-gap engineering. For instance, in a magnetic tunnel junction, electrons that are transmitted from one electrode to the other have to pass the nonconducting spacer.[21] The transmission probability decays with spacer thickness and with the width of the spacer's fundamental band gap.[22,23] As a consequence, the spin-dependent conductance, i.e., the tunnel magnetoresistance, could be tuned by varying the fundamental band gap. Further, the magnetoresistance depends essentially on the properties of the ferromagnet-insulator interface, as was shown for Fe/MgO/Fe tunnel junctions.[24,25] Hence, detailed knowledge of its geometric structure is necessary and our theoretical investigation of the bulk structural phases can be regarded as one step toward that goal.

In addition to the extensive experimental work, there exist many detailed theoretical studies of both ZnO and MgO. Among them are Refs. 26–36, using a variety of *ab initio* computational methods. There are, however, not many stud-

ies of $Mg_xZn_{1-x}O$ alloys, possibly due to the complex interplay of their electronic and geometric structures.[37–43] Recently, thermodynamical stability and ordering tendencies of the alloys have been carefully investigated using the cluster-expansion method.[38] Based on the parameterization of total energies for various alloy configurations, the latter allows to study accurately structural properties, including short-range-order (SRO) effects.[44,45] It is found that the **RS**↔**WZ** transition occurs at $x \approx 0.33$, which is consistent with experiment ($x=0.33$, Ref. 7; similar results were obtained by a pseudopotential method using supercells[37]). The cluster-expansion method was also used by Seko *et al.*[39] for investigating phase transitions, including vibrational effects through lattice dynamics calculations. The authors demonstrate that the transition pressure decreases with increasing Mg content, which is explained as follows. Below the solubility limit of MgO in ZnO, the RS phase is energetically preferred to the WZ phase in MgO. Above the solubility limit, the configurational entropy increases by the transition from a mixed **WZ**-ZnO/**RS**-MgO to a RS single phase. An extensive systematic study of structural properties of $Mg_xZn_{1-x}O$ was performed by Fan *et al.*[41] using a supercell approach within the local-density approximation. They obtained the region of phase stability for $Mg_xZn_{1-x}O$ at $0.375<x<0.5$. Chen *et al.*[42] used the generalized gradient approximation (GGA) and got contradictory structural results to Fan *et al.*, with the transition pressure predicted at $x=0.69$, which is far from experiment ($x=0.4–0.5$).

A brief critical review of previous theoretical *ab initio* investigations has shown that: (i) In ZnO, the energy levels of the localized Zn $3d$ electrons are found relatively high and thus close to the valence bands, resulting in strong hybridization with O $2p$ states. Since these hybridization effects have to be correctly taken into account, the all-electron methods are preferred to the pseudopotential methods in which localized electrons are neglected. (ii) Because the Zn $3d$ electrons are localized, they are not well described within the local spin-density approximation (LSDA) to density-functional theory. To treat these electronic states adequately, one has to go beyond the LSDA, for example, by applying the self-interaction correction (SIC) to the LSDA. (iii) Previous studies often focused on the WZ and RS structures of the ordered alloys (i.e., $x=0$ or 1). A detailed investigation of the complete transition path (with continuous variation in x) is still missing. For the latter it is inevitable to treat disordered alloys, for example, within the coherent-potential approximation.

In the present paper, we report on a systematic first-principles study of structural and electronic properties of ordered and disordered $Mg_xZn_{1-x}O$ alloys using an all-electron full-charge-density Korringa-Kohn-Rostoker (KKR) method.[46,47] Alloying of MgO and ZnO is described within coherent-potential approximation (CPA),[48] as formulated in multiple-scattering theory (KKR-CPA).[49] One objective of this investigation is to describe accurately the structural phase transition from the WZ to the RS structure in $Mg_xZn_{1-x}O$, by continuously increasing the Mg concentration. The second objective addresses the formation of the fundamental band gap in $Mg_xZn_{1-x}O$. It is further shown how the hybridization between Zn $3d$ and O $2p$ states affects the width of the band gap, by comparing results obtained within the LSDA with those obtained by applying the self-interaction correction.[50,51] The validity of the present approach, especially the use of the CPA, is discussed by comparing our results with those of previous studies.[37–39] In summary, our study addresses important issues in $Mg_xZn_{1-x}O$ alloys which, with respect to magnetic tunnel junctions, might also be relevant for magnetoelectronics.

The paper is organized as follows. The model of the transition path from the WZ to the RS structure is sketched in Sec. II. Details of the computational approach are presented in Sec. III. Results are discussed in Sec. IV. By comparing our results for the ordered alloys with those of other theoretical work and with experiment, the validity of our approach has been established. Our main results for the disordered alloys are discussed in Sec. V. In Sec. VI, the formation and evolution of the fundamental band gap as a function of Mg and Zn contents in the system is analyzed. Concluding remarks close the paper in Sec. VII.

II. MODELING THE STRUCTURAL WZ↔RS PHASE TRANSITION

To investigate structural phase transitions in $Mg_xZn_{1-x}O$, a transition path suggested for the continuous structural **WZ**↔**RS** transformation in GaN was adopted.[31] This path has been already successfully applied in studies of structural deformations in MgO (Ref. 32) and in ZnO.[52] The structural transition is described as a homogenous strain deformation from the WZ to the RS phase by passing an intermediate hexagonal structure (HX, referred to as *h*-MgO in Ref. 31). This hexagonal structure can as well occur in epitaxial systems due to the reduction in the interlayer distance, which was recently observed for thin ZnO films.[53,54] A similar scheme is the Bain path for the transition from the face-centered-cubic to the body-centered-cubic structure.[55]

In the first step on the transition path (**WZ**↔**HX**), the internal parameter u is linearly increased while simultaneously decreasing the c/a ratio (Fig. 1). At $u=1/2$ the space group changes from $P6_3mc$ to $P6_3/mmc$. In the second step (**HX**↔**RS**), the lattice is compressed uniaxially along the $[10\bar{1}0]$ direction and simultaneously c/a is decreased further. The WZ phase is characterized by $a=b$, $c/a=\sqrt{8/3}$, $v=1/3$, and $u=3/8$, whereas the HX phase has $a=b$, $c/a=1.2$, $v=1/3$, and $u=1/2$. For the RS phase, $a=b=c$ and $v=u=1/2$. For details, see Ref. 32.

To perform total-energy minimizations (see Sec. III), the appropriate unit cell of an orthorhombic lattice with space group $Cmc2_1$ was used (Fig. 1). The latter is a common subgroup of all three phases.[56] In our calculations, the parameter v, specifying the relative positions of the sublattices[32] and the ratio b/a (defined in Fig. 1) are fixed by the geometry of a particular phase. The parameter u, which is the internal vertical displacement of the cation atoms in the oxygen plane and the c/a ratio were obtained by the total-energy minimization for the pure compounds (i.e., **WZ**-ZnO and **RS**-MgO) within LSDA. They are kept fixed at these values for $Mg_xZn_{1-x}O$ alloys for all concentrations x.

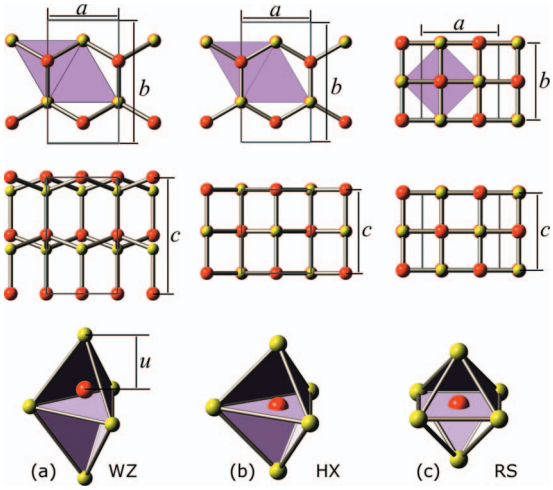

FIG. 1. (Color) Structural phases in $Mg_xZn_{1-x}O$. The wurtzite structure (a: WZ, left column), the intermediate hexagonal structure (b: HX, central column), and the rock-salt structure (c: RS; right column) are shown in top view (top row) and in side view (central row). The respective hexahedral and octahedral chemical units are depicted in the bottom row. The lattice parameters a, b, and c for the common space group $Cmc2_1$ are indicated. The xy plane of unit cells for $P6_3mc$, $P6_3/mmc$, and $Fm\bar{3}m$ space groups for WZ, HX, and RS, respectively, are displayed in the top row in magenta (dark-ish rhombe areas). u describes the internal displacement of cations sites (red, dark spheres) with respect to the central planes of the polyhedra. For $u=1/2$, metal sites lie within the central planes which are spanned by the oxygen sites (yellow, bright spheres).

III. COMPUTATIONAL DETAILS

The electronic and geometric structures of $Mg_xZn_{1-x}O$ alloys are obtained within density-functional theory. The local-density approximation and its self-interaction correction (see below) are implemented in a multiple-scattering approach (the Korringa-Kohn-Rostoker method, KKR).[57] Disordered alloys are described within the coherent-potential approximation.[58]

For closed-packed systems, for example, transition metals, the crystal potential is commonly approximated as a sum over the so-called "muffin-tin potentials"[59] (that is, spherically symmetric potentials centered at each lattice site while in the interstitial region the potential is constant). For open systems, this approximation results in a relatively poor description of the electronic structure. It has turned out that the usual trick of inserting the so-called "empty spheres" into the interstitial region is not sufficient for MgO and ZnO, in particular, in view of the high degree of accuracy needed in the evaluation of total energies. Obviously, the latter is inevitable for a reliable description of structural phase transitions. Consequently, a full-charge-density approximation was applied. Here, the total energy is estimated from the nonspherical charge density and the full potential. All radial integrals are calculated using the unit-cell geometry; the single-site problem is still solved with a spherical potential averaged within a Voronoi cell. The accuracy of this approach is as good as that of a full-potential method but is not as time consuming. The validity of the full-charge-density approximation was checked by comparison with results of the corresponding KKR full-potential calculations for the ordered **WZ**-ZnO and **RS**-MgO compounds.

The disordered $Mg_xZn_{1-x}O$ can be viewed as a substitutional binary alloy in which the metal sublattice (Zn, Mg) is subject to chemical disorder. The oxygen sublattice remains unaffected. Hence, the coherent-potential approximation is an obvious choice for describing $Mg_xZn_{1-x}O$ at an arbitrary concentration x. Within the CPA, Mg and Zn impurities are embedded into an effective coherent-potential medium which is determined self-consistently.[57,58] Since the KKR-CPA is a single-site approximation, it does not allow to investigate the influence of chemical short-range order on the electronic properties (SRO can be taken into account by the cluster CPA,[60] the locally self-consistent Green's-function method[61] or the nonlocal CPA approach[62]). However, for many alloys the single-site CPA provides a reasonable description of the electronic structure.[63] For $Mg_xZn_{1-x}O$, the validity of the KKR-CPA was established through a direct comparison with KKR supercell calculations (which include SRO effects) for $x=0.25$, 0.50, and 0.75. The major structural and electronic properties, such as the equilibrium lattice constants, bulk moduli, equilibrium pressures, and fundamental band gaps, are reproducible within both the KKR-CPA and the supercell approach. Hence we conclude that SRO effects cannot be ruled out but they are of minor importance for the issues addressed in this work. A detailed investigation of SRO effects is beyond the scope of the present work.

Although the Mg $2p$ electron states lie comparably deeply in energy (about 2 Ry below the valence bands), they have been treated as valence states. It is found that the hybridization of the associated electronic states with the valence states is important for an accurate determination of total energies, especially for the evaluation of both the c/a ratio and the parameter u in the WZ structure. The same procedure was applied in an earlier all-electron study of MgO, using a full-potential linearized muffin-tin orbital (FP-LMTO) method.[32]

Since the Zn $3d$ states are energetically close to the O $2p$ states, they have to be considered as valence electrons as well. It is well known that the hybridization of the localized Zn $3d$ electrons with the O $2p$ electrons is crucial for an accurate investigation of the band-gap formation in ZnO.[64] Being strongly localized, the Zn $3d$ states are not adequately described within the local-density approximation. The LSDA contains the (unphysical) self-interaction of an electron with itself (see e.g., Refs. 51 and 65), an effect whose importance increases with the degree of electron localization. As a consequence of the self-interaction, the energy levels of the localized electrons obtained within the LSDA lie too high and their hybridization with the O $2p$ states is too strong. The calculated fundamental band gap in ZnO is therefore considerably too small as compared to experiment.

An improved description of localized electrons is achieved by the self-interaction correction[50,51] in which the unphysical self-interaction is removed from the LSDA exchange-correlation functional. In this approach, SIC is applied to various configurations of localized electron states and the configuration with the lowest total energy defines the ground-state energy and configuration. The SIC-LSD approach, being based on a variational principle, is parameter

free and treats on equal footing both itinerant and localized electrons. When no localized electrons are present in the system, then the SIC-LSDA total energy is equivalent to the LSDA total energy. Thus the LSDA energy functional is a local minimum of the SIC-LSDA functional. For ZnO in both the RS and the WZ phase it is found that all 3*d* electrons have to be SI corrected. Since the Zn 3*d* states have semicore character, application of the SIC leads to a uniform increase in the binding energies of these states, to a decrease in the total energy, and to an increased fundamental band gap in ZnO. Because other electronic states were treated within the LSDA, we label these calculations SIC-LSDA for short.

To check whether SIC affects only the fundamental band gap or also structural properties, we have compared results of a SIC-LSDA calculation for ZnO with those of an LSDA calculation, based on the same computer code. It has been shown that structural properties calculated within both LSDA and SIC-LSDA are very close whereas the band gap obtained within SIC-LSDA has been substantially larger than in the LSDA case. This finding has been further verified for disordered $Mg_xZn_{1-x}O$ alloys at selected concentrations. As a result, in order to save computational costs, only LSDA has been used for the studies of the structural properties. In contrast, here, the fundamental band gap has been investigated at the respective equilibrium lattice constants within SIC-LSDA. For both the LSDA and SIC-LSDA calculations the Perdew-Wang exchange-correlation functional has been applied.[66]

The equilibrium volumes, bulk moduli, pressures, and enthalpies have been calculated for zero temperature from the total energy fitted to the Murnaghan equation of state.[67] Lattice vibrations, finite-temperature effects, and relativistic corrections have not been considered. The angular momentum cutoffs l_{max} have been chosen as 3 for the Green's function expansion and 6 for both the charge-density and the potential representation. The convergence with l_{max} and with normalization of the Green's function was significantly improved by use of Lloyd's formula in this work.[68,69] The concentration, x, of Mg impurities in ZnO has been varied in steps of 5%.

IV. STRUCTURAL PROPERTIES OF ORDERED ZnO AND MgO IN RS AND WZ PHASES

Due to the large number of structural parameters, a complete structure optimization of $Mg_xZn_{1-x}O$ alloys is an involved task. Apart from these parameters, the alloy composition x is an additional degree of freedom which complicates the problem further. Therefore, the number of parameters to be optimized has been reduced by concentrating on volume changes in the WZ, HX, and RS structures upon variation in x (see Sec. II).

TABLE I. Properties of ZnO in the WZ, the HX, and the RS phase. Equilibrium volumes V_0, c/a ratios, internal parameters u, and bulk moduli B_0 are compiled for theoretical (present work displayed as numbers without superscripted references) and for experimental works. PPW, PAW, LCAO, FP-LMTO, and FP-(L)APW+lo are abbreviations for pseudopotential plane waves, projector-augmented wave, linear combination of atomic orbitals, full-potential linearized muffin-tin orbital, and full-potential (linearized) augmented plane-wave and local orbitals, respectively. Parametrization: PW92 (present work) – Perdew-Wang 92 functional (Ref. 66), T – Teter (Ref. 70), VWN – Vosko-Wilk-Nussair (Ref. 71), CA – Ceperley-Alder (Ref. 72), HL – Hedin-Lundqvist (Ref. 73), and PW91 – Perdew-Wang 91 GGA functional (Ref. 74).

Phase		Theory	Experiment
WZ	V_0 (Å^3)	22.83, 22.80[a], 22.83[b], 22.89[c], 22.87[d], 22.91[e], 22.93[f], 23.40[g], 23.62[h], 23.78[i], 24.67[j]	23.80[l], 23.81[k]
	c/a	1.601, 1.590[h], 1.604[b], 1.605[i], 1.607[e], 1.608[g], 1.610[a], 1.614[d], 1.615[c], 1.617[f]	1.601[l], 1.602[k]
	u	0.380, 0.379[d], 0.380[a,g,h], 0.381[b,e]	0.382[k]
	B_0 (GPa)	154, 154[i], 155[e], 157[g], 160[h], 162[a,d,f]	143[k], 183[l]
HX	V_0 (Å^3)	22.12	
	c/a	1.200	
	B_0 (GPa)	165	
RS	V_0 (Å^3)	18.88, 18.67[b], 18.70[a], 18.76[e], 18.87[f], 18.90[d], 19.08[h], 19.45[i], 20.30[j]	19.48[l], 19.60[k]
	B_0 (GPa)	201, 200[i], 203[e], 206[d], 210[a], 211[f], 219[h]	203[k], 228[l]

[a]Reference 52: PPW.
[b]Reference 41: PAW.
[c]Reference 40: PPW, T.
[d]Reference 30: LCAO, VWN.
[e]Reference 36: LCAO, VWN.
[f]Reference 39: PPW, CA.
[g]Reference 75: FP-LMTO.
[h]Reference 76: FP-LMTO, HL.
[i]Reference 37: PPW, CA.
[j]Reference 42: PAW, PW91.
[k]Reference 27.
[l]Reference 77.

TABLE II. As Table I but for MgO.

Phase		Theory	Experiment
WZ	V_0 (Å^3)	23.20, 22.50[g], 22.54[e], 22.68[a], 22.74[f], 23.15[d]	
	c/a	1.601, 1.486[a], 1.550[e], 1.620[g], 1.633[d]	
	u	0.380, 0.375[d,g] 0.405[a]	
	B_0 (GPa)	121, 131[e], 137[g]	
HX	V_0 (Å^3)	21.71, 20.73[d], 20.90[g]	
	c/a	1.200, 1.200[g], 1.204[d]	
	B_0 (GPa)	135, 148[d,g]	
RS	V_0 (Å^3)	18.19, 17.55[e], 17.80[d,g], 17.89[a], 17.96[c], 18.03[b], 18.05[h], 18.10[i], 18.11[j], 18.65[k], 19.06[f]	18.67[l], 18.75[m]
	B_0 (GPa)	167, 169[i], 170[e], 171[h], 172[k], 174[c], 178[d,g], 186[b]	169[n], 172[o]

[a]Reference 41: PAW.
[b]Reference 30: LCAO, VWN.
[c]Reference 39: PPW, CA.
[d]Reference 75: FP-LMTO.
[e]Reference 37: PPW, CA.
[f]Reference 42: PAW, PW91.
[g]Reference 32: FP-LMTO, HL.
[h]Reference 78: FP-LMTO, PW92.
[i]Reference 78: PAW, PW92.
[j]Reference 79: FP-(L)APW+lo, PW92.
[k]Reference 33: FP-KKR.
[l]Reference 80.
[m]Reference 81.
[n]Reference 82.
[o]Reference 83.

To our knowledge, the KKR method was not used before for optimizing WZ and HX structures. Hence extensive calculations for pure ZnO and MgO have been required to determine both the optimum u and c/a. In accomplishing this, the procedure suggested in Ref. 32 has been followed. Since the calculation of lattice relaxations from forces is rather complicated and not sufficiently accurate within the KKR method, we have calculated the total energies consecutively varying three parameters: the lattice constants a, the c/a, and the internal parameter u. The total energy has been calculated at a given u for a sufficiently dense mesh of lattice constants and then fitted to the Murnaghan equation of state. The initial value of the parameter u has been taken from the experiment for a particular structure and then successively varied as long as the absolute total-energy minimum has not been reached. To establish the validity of the present KKR approach for structure optimization, our results have been compared with those of other first-principles calculations. We note that our calculations for both ZnO and MgO in various structures have been carried out for the same unit cell on the same level of approximation.

The adequacy of the present approach can be established through comparison with the experimental data and results of other theoretical approaches summarized in Tables I and II. Overall, the agreement of our results with experiment and other approaches is good or even very good, as in the case of ZnO, when compared with the pseudopotential plane waves (PPW) approach (see Table I). The agreement of our results with the other all-electron calculations, e.g., those reported by Limpijumnong and coworkers,[32,52] using a FP-LMTO method, is not always as good. This is perhaps slightly surprising considering that, in addition, both studies followed the same optimization scheme (as implemented in Refs. 32 and 52) and that the Zn $3d$ as well as the Mg $2p$ electrons have been treated as valence electrons.

As for the structural properties, we find agreement concerning the volume ratios of the different phases and the equilibrium pressures at the phase transitions (see Tables III and IV). For ZnO there is only the **WZ**↔**RS** phase transition while for MgO there are two transitions, namely, **RS**↔**HX** and **RS**↔**WZ**. In particular, for ZnO, our theoretical results compare well with experimental ones (see Table III). For MgO we find agreement with other theoretical estimations too (Table IV). However, the equilibrium pressure for the RS-HX phase transition might be an exception. The apparent disagreement with the result reported in Ref. 32 may be related to the instabilities of the WZ and the HX structures [Figs. 2 and 3(a)]. Moreover, due to the negative pressure these phases cannot be realized experimentally, hence ruling out a clarifying comparison of theory with experiment. In favor of our work, we would like to mention that the present calculations reproduce well c/a and u. One might speculate that earlier implementations of multiple-scattering theory failed to optimize these structural parameters in any open structure due to the slow angular momentum convergence of the Green's function (see Sec. III; the convergence is significantly improved by using Lloyd's formula).[84]

In summary, the agreement of our results for the ordered alloys with those of other theoretical investigations and experiments indicates that the present approach is as reliable and accurate as any other state-of-the-art methods.

V. STRUCTURAL PROPERTIES OF DISORDERED $Mg_xZn_{1-x}O$ ALLOYS

Having established that our results for ordered ZnO and MgO are consistent with the structural properties obtained by

TABLE III. Structural phase transition in ZnO. Given are the volume ratio and the equilibrium pressure at the **WZ**↔**RS** phase transition. Present work is displayed by numbers without the superscripted references.

	Theory	Experiment
$V_{\mathbf{WZ}}/V_{\mathbf{RS}}$	1.21, 1.21[c], 1.22[b,d,e,g,h], 1.24[f]	1.21[i], 1.22[j]
$P_{\mathbf{WZ}\leftrightarrow\mathbf{RS}}$ (GPa)	8.6, 3.9[d], 6.6[c], 8.0[f], 8.2[a], 8.7[e]	8.7[j], 9.1[i]

[a]Reference 52: PPW.
[b]Reference 41: PAW.
[c]Reference 30: LCAO, VWN.
[d]Reference 36: LCAO, VWN.
[e]Reference 39: PPW, CA.
[f]Reference 76: FP-LMTO, HL.
[g]Reference 37: PPW, CA.
[h]Reference 42: PAW, PW91.
[i]Reference 27.
[j]Reference 77.

other theoretical methods and by experiments, we now turn to the discussion of results for disordered $Mg_xZn_{1-x}O$ alloys. To reduce the number of parameters to be optimized, both c/a and u were fixed, respectively, to 1.6 and 0.38 in the WZ structure and to 1.2 and 0.5 in the HX structure. This approximation is justified by the weak dependence of both c/a and u on the atomic species (Mg or Zn; cf. Tables I and II). Consequently, the structure (the actual phase), Mg concentration x, and unit-cell volume remain to be varied. The results of the total-energy calculations involving these three variables are discussed below. The results of the total-energy calculations are comprised in the energy of formation, which is equal to enthalpy in equilibrium (at $T=0$)

$$\Delta H_\alpha(Mg_xZn_{1-x}O) = E_\alpha(Mg_xZn_{1-x}O) - xE_{\mathbf{RS}}(MgO) - (1-x)E_{\mathbf{WZ}}(ZnO) \quad (1)$$

of a structure α of $Mg_xZn_{1-x}O$, relative to the most stable forms of MgO (RS) and ZnO (WZ) compounds, weighted respectively by x and $1-x$.[38]

The energy of formation is positive throughout, as seen in Fig. 2, in agreement with previous theoretical studies.[38,39] Our CPA calculations agree well with our supercell calculations performed for $x=0.25$, 0.5, and 0.75, and for other concentrations x also with the calculations of Fan *et al.*[41] There are two global minima (i.e., the most stable phases; black, dark regions), for pure ZnO in WZ ($x=0$) and pure MgO in RS phase ($x=1$). This finding implies a tendency toward phase separation if the integration of different constituents into the medium cannot be maintained.[38]

TABLE IV. As Table III but for MgO. For MgO there are two transitions, **RS**↔**HX** and **RS**↔**WZ**. Experimental data are not available. Present work is displayed by numbers without the superscripted references.

	Theory
$V_{\mathbf{HX}}/V_{\mathbf{RS}}$	1.19, 1.17[d]
$P_{\mathbf{RS}\leftrightarrow\mathbf{HX}}$ (GPa)	−8.5, −16.2 [d]
$V_{\mathbf{WZ}}/V_{\mathbf{RS}}$	1.24, 1.19[c], 1.26[d], 1.27[a], 1.28[b]
$P_{\mathbf{RS}\leftrightarrow\mathbf{WZ}}$ (GPa)	−11.1, −8.4[d]

[a]Reference 41: PAW.
[b]Reference 37: PPW, CA.
[c]Reference 42: PAW, PW91.
[d]Reference 32: FP-LMTO, HL.

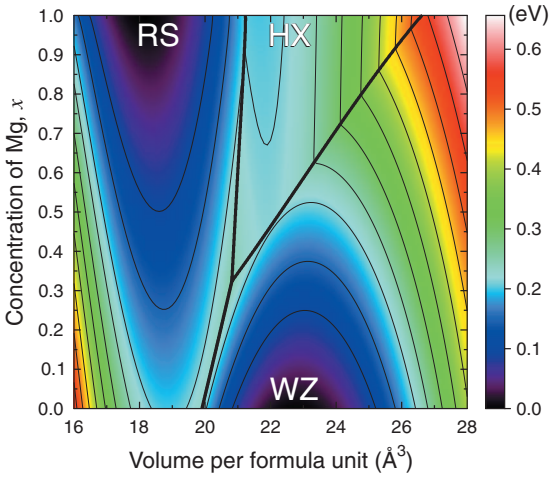

FIG. 2. (Color) Energy of formation per formula unit of $Mg_xZn_{1-x}O$ alloys versus equilibrium volume and Mg concentration, depicted as color scale [cf. eq. (1)]. Straight bold lines mark separations between the phases (WZ, HX, and RS).

In the following, five special cases are discussed in more detail, namely, $x=0.0$, 0.33, 0.52, 0.71, and 1.0, and summarized in Table V.

For low Mg concentrations, the WZ phase is favorable [Fig. 3(a)] and the pressure needed for a **WZ**↔**RS** transition is positive but decreases monotonously with increasing Mg concentration and from $x\geq 0.33$ switches to negative values, as the RS phase becomes the favourable one. (Fig. 4).

For $x<0.33$ the total energy of the HX structure is higher than for the RS and the WZ phases, implying that an intermediate HX phase cannot be established (Fig. 2). Conse-

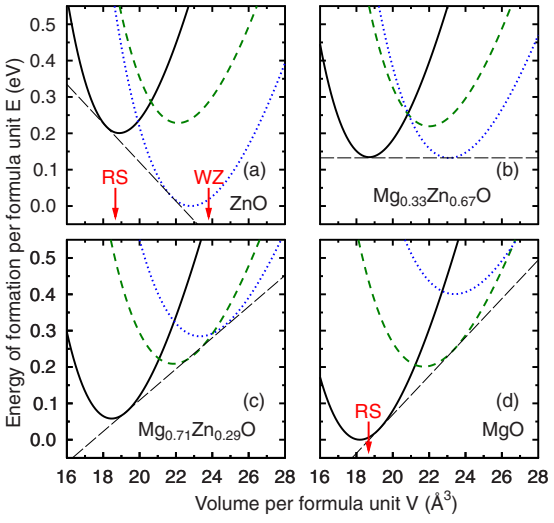

FIG. 3. (Color online) Energy of formation per formula unit of $Mg_xZn_{1-x}O$ alloys in RS (black solid line), HX (green dashed line), and WZ (blue dotted line) structures at four different concentrations: (a) $x=0.0$ (pure ZnO), (b) $x=0.33$, (c) $x=0.71$, and (d) $x=1.0$ (pure MgO). Red arrows mark the respective experimental volumes (see Tables I and II).

TABLE V. Summary of the structural properties and transition pressures calculated here for $Mg_xZn_{1-x}O$ alloys.

Conditions		Properties
$x=0$	$P=8.58$ GPa	Phase transition **WZ**↔**RS**
$x=0.33$	$P=0$	Two phases possible: **WZ**↔**RS**
$x\geq 0.33$		**HX** phase occurs
$x=0.52$		Local minima: $E^{\min}_{\mathbf{WZ}}=E^{\min}_{\mathbf{HX}}$
$x=0.71$	$P=-7.02$ GPa	Double phase transition
		RS↔**HX**↔**WZ**
$x=1$	$P=-8.51$ GPa	Phase transition **RS**↔**WZ**

quently, a direct **WZ**↔**RS** transition is possible at positive pressure. At $x=0.33$ [Figs. 3(b) and 5] this phase transition can take place at zero pressure. This finding is consistent with the theoretical work of Sanati and coworkers[38] and is also observed experimentally in ZnO-MgO heterostructures.[7]

At $x=0.71$ the **WZ**↔**HX** and the **HX**↔**RS** transitions occur at the same pressure (Fig. 4). This is evident from Fig. 3(c) because all total-energy curves can be connected by a single tangent. We note that for $x=0.52$ the **WZ**↔**HX** transition is possible at zero pressure and the corresponding total energies relative to RS phase are identical (see Fig. 5).

For pure MgO [$x=1.0$; Fig. 3(d)], the RS structure exhibits the global minimum at a volume of 18.19 Å^3 which is about 2% less than the experimental value (see Table II). By applying a negative pressure (i.e., by increasing the volume along the tangent) the RS phase is transformed into the HX structure, in agreement with the work of Limpijumnong and coworkers.[32]

According to the phase diagram (Fig. 2), the HX phase is an intermediate phase between the WZ and RS structure for $0.33\leq x\leq 1.00$. The **HX**↔**RS** transition pressure decreases with increasing Mg content and is negative for the whole range of concentrations (Fig. 4).

VI. BAND GAP IN $Mg_xZn_{1-x}O$ ALLOYS

Since $Mg_xZn_{1-x}O$ alloys arouse great interest as band-gap-engineering materials, in this section we study the evolution of their fundamental band gap as a function of the Zn and Mg contents. We restrict our consideration to the RS and WZ phases, as only these appear interesting from the experimental point of view.

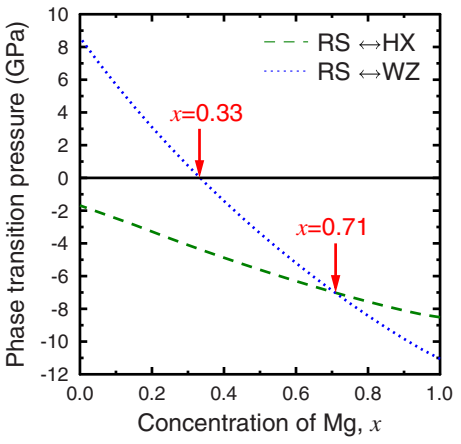

FIG. 4. (Color online) Equilibrium pressure in $Mg_xZn_{1-x}O$ alloys: **RS**↔**HX** (green dashed line) and **RS**↔**WZ** (blue dotted line).

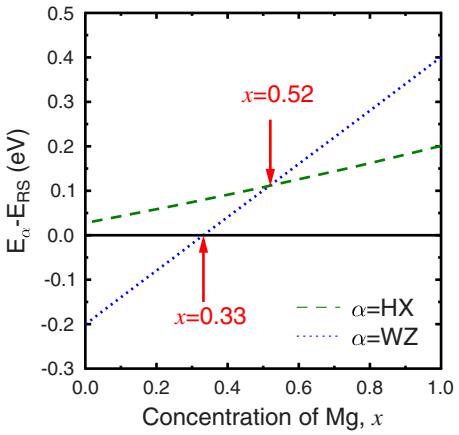

FIG. 5. (Color online) Total energies of $Mg_xZn_{1-x}O$ alloys in the HX (green dashed line) and the WZ (blue dotted line) structures, taken relative to the total energy of the RS structure at equilibrium volumes.

Band-gap formation can be correctly described only within a many-body theory which takes properly into account the electron-hole excitations. However, the GW approximation,[85] probably the most popular first-principles many-body approach for calculating excitation energies, is too expensive for studying alloys with arbitrary concentrations and also having constituents with localized electrons. Therefore, for this study we have used only the LSDA and SIC-LSDA approaches. The calculated band gaps have been estimated from the density of states (DOS), band structure and Bloch spectral function, corresponding to the theoretical equilibrium lattice structure of a given chemical composition.

Using LSDA for **RS**-MgO we obtain a band gap of 5.15 eV, which is 67% of the experimental value (7.7 eV). For the pure **WZ**-ZnO, LSDA gives the band gap of 0.8 eV, which is only 23% of the experimental value of 3.35 eV. In MgO, the difference between the calculated and experimental values originates from the fact that in LSDA there is no contribution to the band gap from the derivative discontinuity of the exchange-correlation potential.[86–88] This failure can be effectively corrected with the GW approximation.[89] For ZnO the problem is more complex as, in addition, the localized nature of Zn $3d$ electrons is not adequately represented within LSDA. This failure of LSDA is largerly related to the inherent unphysical self-interaction. The latter affects the band gap by placing the localized $3d$ electrons of Zn at too low binding energies, thus leading to their strong hybridization with the O $2p$ states. In LSDA the Zn $3d$ states are about 3 eV too high with respect to the experimental value of about 7.5–8.5 eV (Refs. 90 and 91) (see the DOS of ZnO in Fig. 6). In the RS and WZ phases, the $3d$ states are placed at slightly different energies, and in the RS the corresponding band width is larger due to the more closed-packed crystal environment. The strong pd hybridization dramatically reduces the band gap, which can be improved only slightly within the

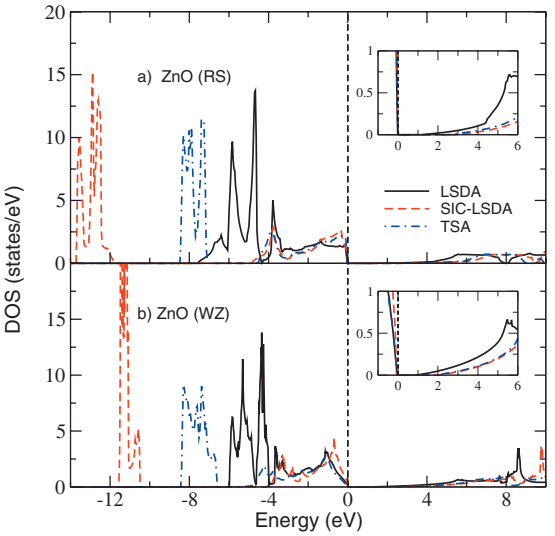

FIG. 6. (Color) DOS of ZnO in (a) the RS and (b) the WZ phase obtained with the LSDA (black solid lines), the SIC-LSDA (red dashed lines), and SIC-TSA (blue dash-dotted lines) approaches. Insets show the behavior of the DOS and fundamental band gap close to the Fermi level. The energy is given relative the Fermi level.

GW approximation, if based on the LSDA Green's function.[64] It is the aim of our future studies to use the SIC-LSDA band structure of ZnO for the subsequent GW calculation.

The SIC-LSDA band gap we have calculated is 2.42 eV for **WZ**-ZnO and 2.96 eV for **RS**-ZnO. Thus, the SIC-LSDA band gap for the **WZ**-ZnO constitutes 69% of the experimental value of 3.35 eV. This tells us that SIC-LSDA is at least as good for the pure ZnO, as LSDA is for the pure MgO. The reason being, that SIC-LSDA describes both itinerant and localized electrons on equal footing. Also, since SIC-LSDA is an orbital-dependent theory, it has the mechanism of the derivative discontinuity of the exchange-correlation potential built in it. However, whether its effect on the magnitude of the gap is direct or indirect depends on how much the states involved in establishing the band-gap benefit from the self-interaction correction. In MgO the band gap is constituted by the *sp* electrons which are itinerant and thus unaffected by the spurious self-interaction while in ZnO the 3*d* electrons of Zn play a defining role in establishing the band gap. The SIC-LSDA approach, by removing the unphysical self-interaction of all ten Zn *d* electrons, describes them more adequately than LSDA. What happens as a result of SIC is that all the *d* states of Zn move to higher binding energies and the Zn-derived bands become narrower thereby reducing the *pd* hybridization and increasing the band gap, as seen in Fig. 6. The structural properties of $Mg_xZn_{1-x}O$ are believed to be little affected by this uniform shift downward in energy of the *d* states, leading mostly to a uniform lowering of the total energy.

Being an effective one-electron ground-state theory, SIC-LSDA does not provide a quasiparticle spectrum to compare with spectroscopies. Missing the crucial screening/relaxation effects (self-energy), it predicts the 3*d* Zn electrons at too high binding energies, as opposed to LSDA where they come

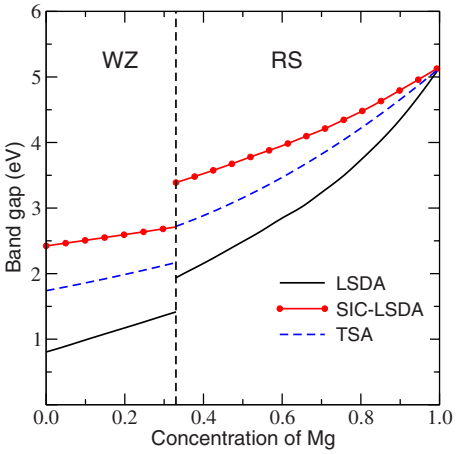

FIG. 7. (Color online) Band gaps of $Mg_xZn_{1-x}O$ alloys in the RS and WZ phases versus Mg content, calculated within LSDA and SIC-LSDA (line styles as indicated).

out too low (Fig. 6). One can implement a simple procedure to correct for the screening effects in SIC-LSDA, inspired by the Slater transition state theory.[92,93] Following the arguments of the latter in relation to SIC,[94] and assuming a linear behaviour of the single-particle energies with occupation numbers, we calculate the SIC-LSDA-based removal energies of localized electrons as

$$\varepsilon_{\mathrm{TSA}} = \frac{1}{2}(\langle d|H_{\mathrm{LSDA}} + V_{\mathrm{SIC}}|d\rangle + \langle d|H_{\mathrm{LSDA}}|d\rangle). \qquad (2)$$

Effectively, the above equation states that only half of the SIC potential should be applied at the stage of calculating the density of states, after the self-consistency has been achieved. We refer to Eq. (2) as the transition state approximation (TSA) and show the resulting DOS of ZnO in Fig. 6. We can see that Zn *d* states, calculated using TSA, appear at lower binding energies, as compared to the strict SIC-LSDA result. Consequently, the TSA-binding energies of Zn *d* states are in better agreement with experimental values of 7.5–8.5 eV.[90,91] The effective hybridization of Zn *d* states with the oxygen *p* states is stronger than in the SIC-LSDA case, which leads to a reduction in the band gap to 2.32 and 1.74 eV (52% of the experimental value) in RS and WZ phases, respectively.

In $Mg_xZn_{1-x}O$ alloys the size of the band gap depends on the concentration of Mg impurities, as seen in Fig. 7 and Table VI. While at the Mg rich end the LSDA band gaps are closer to experiment, at the other end the SIC-LSDA band gaps are more adequate. As for the TSA results, they fall mostly in between the LSDA and SIC-LSDA band gaps, especially for small Mg concentrations, where the hybridization of the O 2*p* bands with the Zn 3*d* states is of great significance (see Fig. 7). The behavior of the band gap as a function of Mg concentration is also different between the various approaches. While the LSDA curves are rather parabolic, the SIC-LSDA and TSA band gaps seem to change almost linearly with concentration, thus following more closely experimental results.[18,19] This is mostly due to the fact that the actual magnitudes of the band gaps change

TABLE VI. The band gap E_g for MgO(**RS**), ZnO(**WZ**) and the bowing parameter for $Mg_xZn_{1-x}O$ alloys.

	LSDA	TSA	SIC-LSDA	Experiment
		Band gap (eV)		
RS-MgO	5.15			7.70
WZ-ZnO	0.80	1.74	2.42	3.35
		Bowing parameter (eV)		
RS	1.90	0.91	0.59	0.70 ± 0.2 [a]
WZ	4.88	4.05	3.65	3.60 ± 0.6 [b]

[a]Reference 18: PPW.
[b]Reference 19: PAW.

slower with concentration in SIC-LSDA and TSA than in LSDA. The reason being that the larger Zn content, the more inadequate LSDA is and the smaller the resulting band gaps.

Although, both LSDA and SIC-LSDA underestimate the size of the band gap, E_g, its dependence on the Mg concentration, x, can be compared with experimental results. One way of doing it is to estimate the so-called bowing parameter, b, appearing in the commonly used definition of the fundamental band-gap dependence on the composition x, namely,

$$E_g(x) = xE_g(\mathrm{MgO}) + (1-x)E_g(\mathrm{ZnO}) - bx(1-x),$$

where the bowing parameter is given by

$$b = 2E_g(\mathrm{MgO}) + 2E_g(\mathrm{ZnO}) - 4E_g(\mathrm{Zn_{0.50}Mg_{0.50}O}). \quad (3)$$

Thus to evaluate the bowing parameter one needs to know the band gaps of the pure MgO(**RS**) and ZnO(**WZ**), as well as their alloy with the concentration $x=0.5$.

According to our total-energy calculations the $Mg_xZn_{1-x}O$ at $x=0.5$ occurs in the RS phase which is in agreement with the experiment of Chen *et al.*[18] However, the crystal structure of $Mg_xZn_{1-x}O$ thin-film alloys depends strongly on the method of growth. In variance to Ref. 18, the $Mg_xZn_{1-x}O$ films with $x \leq 0.53$, prepared with the PLD procedure, were found to have the WZ structure. Therefore, for direct comparison with the experiments we have used $Mg_{0.50}Zn_{0.50}O$ in both RS and WZ phases. The resulting calculated bowing parameters for $Mg_xZn_{1-x}O$ alloys are presented in Table VI. We can see that the LSDA systematically overestimates the bowing parameter for both structures while the straight SIC-LSDA agrees very well with experiments. The TSA results fall in between the LSDA and SIC-LSDA values.

Summarizing this section, we have to say that despite rather good agreement of our SIC-LSD bowing parameter with experiments, to be truly predictive, one would need a more robust method such as a combination of SIC and GW. This way we could also predict the correct magnitudes of the band gaps and enter the serious business of band-gap engineering.

VII. CONCLUSIONS AND OUTLOOK

Structural phase transitions and the fundamental band gaps of $Mg_xZn_{1-x}O$ alloys have been investigated by detailed first-principles calculations. The multiple-scattering theoretical approach used here (Korringa-Kohn-Rostoker method) allows to treat disordered alloys within the coherent-potential approximation, that is, $Mg_xZn_{1-x}O$ alloys with arbitrary Mg concentration x, with an accuracy as good as in other first-principles methods. The importance of treating localized states of ZnO appropriately within the framework of the local-density approximation to density-functional theory is established, thereby confirming the usefulness of the self-interaction correction.

The delicate interplay of geometry and electronic structure is not only of importance for bulk systems, as shown in this work. In nanotechnology, interfaces and surfaces play an essential role. Therefore, a correct description of disordered alloys and their electronic structure, in particular, at the Fermi energy, is necessary for predicting material properties, besides confirming and explaining experimental results. However, to be fully predictive regarding the properties of such systems as $Mg_xZn_{1-x}O$ alloys, of importance for device applications, one needs a first-principles approach such as a combination of GW with SIC-LSDA.

ACKNOWLEDGMENTS

This work is supported by the *Sonderforschungsbereich* SFB 762, "Functionality of Oxidic Interfaces." Research at the Oak Ridge National Laboratory was sponsored by the Division of Materials Sciences and Engineering, Office of Basic Energy Sciences, U.S. Department of Energy under Contract No. DE-AC05-00OR22725 with UT-Battelle, LLC. We gratefully acknowledge H. L. Meyerheim for many stimulating discussions. Also, many thanks to Axel Svane for useful discussions and communications. The calculations were performed at the John von Neumann Institute in Jülich and Rechenzentrum Garching of the Max Planck Society (Germany).

*aernst@mpi-halle.de

[1] U. Özgur, Y. I. Alivov, C. Liu, A. Teke, M. A. Reshchikov, S. Doğan, V. Avrutin, S.-J. Cho, and H. Morkoç, J. Appl. Phys. **98**, 041301 (2005).
[2] N. B. Chen and C. H. Cui, Mater. Sci. Eng., B **126**, 16 (2006).
[3] E. R. Segnit and A. E. Holland, J. Am. Ceram. Soc. **48**, 409 (1965).
[4] S. Raghavan, J. P. Hajrab, G. N. K. Iyengarb, and K. P. Abrahamc, Thermochim. Acta **189**, 151 (1991).
[5] A. N. Baranov, V. L. Solozhenko, C. Chateau, G. Bocquillon, J.

P. Petitet, G. N. Panin, T. W. Kang, R. V. Shpanchenko, E. V. Antipov, and Y. J. Oh, J. Phys.: Condens. Matter **17**, 3377 (2005).
[6] V. L. Solozhenko, A. N. Baranov, and V. Z. Tukevich, Solid State Commun. **138**, 534 (2006).
[7] A. Ohtomo, M. Kawasaki, T. Koida, K. Masubuchi, H. Koinuma, Y. Sakurai, Y. Yoshida, T. Yasuda, and Y. Segawa, Appl. Phys. Lett. **72**, 2466 (1998).
[8] A. K. Sharma, J. Narayan, J. F. Muth, C. W. Teng, C. Jin, A. Kvit, R. M. Kolbas, and O. W. Holland, Appl. Phys. Lett. **75**, 3327 (1999).
[9] S. Choopun, R. D. Vispute, W. Yang, R. P. Sharma, T. Venkatesan, and H. Shen, Appl. Phys. Lett. **80**, 1529 (2002).
[10] J. Narayan, A. K. Sharma, A. Kvit, C. Jin, J. F. Muth, and O. W. Holland, Solid State Commun. **121**, 9 (2001).
[11] M. Kunisu, I. Tanaka, T. Yamamoto, T. Suga, and T. Mizoguchi, J. Phys.: Condens. Matter **16**, 3801 (2004).
[12] W. I. Park, G. C. Yi, and H. M. Jang, Appl. Phys. Lett. **79**, 2022 (2001).
[13] T. Takagi, H. Tanaka, S. Fujita, and S. Fujita, Jpn. J. Appl. Phys., Part I **42**, L401 (2003).
[14] S. Fujita, T. Takagi, H. Tanaka, and S. Fujita, Phys. Status Solidi B **241**, 599 (2004).
[15] Z. Vashaei, T. Minegishi, T. Suzuki, M. W. Cho, T. You, and A. Setiawan, J. Appl. Phys. **98**, 054911 (2005).
[16] P. Bhattacharya, R. R. Das, and R. S. Katiyar, Appl. Phys. Lett. **83**, 2010 (2003).
[17] L. A. Bendersky, I. Takeuchi, K.-S. Chang, W. Yang, S. Hullavarad, and R. D. Vispute, J. Appl. Phys. **98**, 083526 (2005).
[18] N. B. Chen, H. Z. Wu, D. J. Qiu, T. N. Xu, J. Chen, and W. Z. Shen, J. Phys.: Condens. Matter **16**, 2973 (2004).
[19] R. Schmidt-Grund, D. Fritsch, B. Schubert, M. Rheinländer, H. Schmidt, H. Hochmut, M. Lorenz, D. Spemann, C. M. Herzinger, and M. Grundmann, *Physics of Semiconductors: 27th International Conference on the Physics of Semiconductors–ICPS-27*, AIP Conf. Proc. Vol. 772, (AIP, New York, 2005), p. 201.
[20] J. Chen, W. Z. Shen, N. B. Chen, D. J. Qiu, and H. Z. Wu, J. Phys.: Condens. Matter **15**, L475 (2003).
[21] S. Datta, *Electronic Transport in Mesoscopic Systems* (Cambridge University Press, Cambridge, 1995).
[22] P. H. Dederichs, P. Mavropoulos, O. Wunnicke, N. Papanikolaou, V. Bellini, R. Zeller, V. Drchal, and J. Kudrnovský, J. Magn. Magn. Mater. **240**, 108 (2002).
[23] X.-G. Zhang and W. H. Butler, J. Phys.: Condens. Matter **15**, R1603 (2003).
[24] X.-G. Zhang, W. H. Butler, and A. Bandyopadhyay, Phys. Rev. B **68**, 092402 (2003).
[25] C. Tusche, H. L. Meyerheim, N. Jedrecy, G. Renaud, A. Ernst, J. Henk, P. Bruno, and J. Kirschner, Phys. Rev. Lett. **95**, 176101 (2005).
[26] J. E. Jaffe and A. C. Hess, Phys. Rev. B **48**, 7903 (1993).
[27] S. Desgreniers, Phys. Rev. B **58**, 14102 (1998).
[28] J. M. Recio, M. A. Blanco, V. Luaña, R. Pandey, L. Gerward, and J. S. Olsen, Phys. Rev. B **58**, 8949 (1998).
[29] N. A. Hill and U. Waghmare, Phys. Rev. B **62**, 8802 (2000).
[30] J. E. Jaffe, J. A. Snyder, Z. Lin, and A. C. Hess, Phys. Rev. B **62**, 1660 (2000).
[31] S. Limpijumnong and W. R. L. Lambrecht, Phys. Rev. Lett. **86**, 91 (2001).
[32] S. Limpijumnong and W. R. L. Lambrecht, Phys. Rev. B **63**, 104103 (2001).
[33] A. N. Baranov, V. S. Stepanyuk, W. Hergert, A. A. Katsnelson, A. Settels, R. Zeller, and P. H. Dederichs, Phys. Rev. B **66**, 155117 (2002).
[34] J. Sun, H.-T. Wang, J. He, and Y. Tian, Phys. Rev. B **71**, 125132 (2005).
[35] R. Laskowski and N. E. Christensen, Phys. Rev. B **73**, 045201 (2006).
[36] J. Uddin and G. E. Scuseria, Phys. Rev. B **74**, 245115 (2006).
[37] E.-C. Lee, Y.-S. Kim, and K. J. Chang, J. Korean Phys. Soc. **39**, S23 (2001).
[38] M. Sanati, G. L. W. Hart, and A. Zunger, Phys. Rev. B **68**, 155210 (2003).
[39] A. Seko, F. Oba, A. Kuwabara, and I. Tanaka, Phys. Rev. B **72**, 024107 (2005).
[40] A. Malashevich and D. Vanderbilt, Phys. Rev. B **75**, 045106 (2007).
[41] X. F. Fan, H. D. Sun, Z. X. Shen, J.-L. Kuo, and Y. M. Lu, J. Phys.: Condens. Matter **20**, 235221 (2008).
[42] X. Chen and J. Kang, Semicond. Sci. Technol. **23**, 025008 (2008).
[43] K.-F. Lin, C.-J. Pan, and W.-F. Hsieh, Appl. Phys. A: Mater. Sci. Process. **94**, 167 (2009).
[44] A. Zunger, in *Statics and Dynamics of Alloys Phase Transition*, edited by P. E. A. Turchi and A. Gonis (Plenum, New York, 1994), p. 361.
[45] D. B. Laks, L. G. Ferreira, S. Froyen, and A. Zunger, Phys. Rev. B **46**, 12587 (1992).
[46] J. Korringa, Physica (Amsterdam) **13**, 392 (1947).
[47] W. Kohn and N. Rostoker, Phys. Rev. **94**, 1111 (1954).
[48] P. Soven, Phys. Rev. **156**, 809 (1967).
[49] B. L. Gyorffy, Phys. Rev. B **5**, 2382 (1972).
[50] J. P. Perdew and A. Zunger, Phys. Rev. B **23**, 5048 (1981).
[51] M. Lüders, A. Ernst, M. Däne, Z. Szotek, A. Svane, D. Ködderitzsch, W. Hergert, B. L. Györffy, and W. M. Temmerman, Phys. Rev. B **71**, 205109 (2005).
[52] S. Limpijumnong and S. Jungthawan, Phys. Rev. B **70**, 054104 (2004).
[53] C. Tusche, H. L. Meyerheim, and J. Kirschner, Phys. Rev. Lett. **99**, 026102 (2007).
[54] H. L. Meyerheim, C. Tusche, A. Ernst, S. Ostanin, I. V. Maznichenko, K. Mohseni, N. Jedrecy, J. Zegenhagen, J. Roy, I. Mertig, and J. Kirschner, Phys. Rev. Lett. **102**, 156102 (2009).
[55] P. M. Marcus, F. Jona, and S. L. Qiu, Phys. Rev. B **66**, 064111 (2002).
[56] H. Sowa, Acta Crystallogr. **A57**, 176 (2001).
[57] *Electron Scattering in Solid Matter*, edited by J. Zabloudil, R. Hammerling, L. Szunyogh, and P. Weinberger (Springer, Berlin, 2005).
[58] A. Gonis, *Green Functions for Ordered and Disordered Systems*, Studies in Mathematical Physics Vol. 4 (North-Holland, Amsterdam, 1992).
[59] P. Weinberger, *Electron Scattering Theory of Ordered and Disordered Matter* (Clarendon, Oxford, 1990).
[60] P. Weinberger, R. Dirl, A. M. Boring, A. Gonis, and A. J. Freeman, Phys. Rev. B **37**, 1383 (1988).
[61] I. A. Abrikosov, S. I. Simak, B. Johansson, A. V. Ruban, and H. L. Skriver, Phys. Rev. B **56**, 9319 (1997).
[62] D. A. Rowlands, A. Ernst, B. L. Györffy, and J. B. Staunton,

Phys. Rev. B **73**, 165122 (2006).
[63] I. A. Abrikosov and B. Johansson, Phys. Rev. B **57**, 14164 (1998).
[64] M. Usuda, N. Hamada, T. Kotani, and M. van Schilfgaarde, Phys. Rev. B **66**, 125101 (2002).
[65] W. M. Temmerman, A. Svane, Z. Szotek, and H. Winter, in *Electronic Density Functional Theory: Recent Progress and New Directions*, edited by J. F. Dobson, G. Vignale, and M. P. Das (Plenum, New York, 1998), p. 327.
[66] J. P. Perdew and Y. Wang, Phys. Rev. B **45**, 13244 (1992).
[67] F. D. Murnaghan, Proc. Natl. Acad. Sci. U.S.A. **30**, 244 (1944).
[68] P. Lloyd, Proc. Phys. Soc. London **90**, 207 (1967).
[69] R. Zeller, J. Phys.: Condens. Matter **16**, 6453 (2004).
[70] S. Goedecker, M. Teter, and J. Hutter, Phys. Rev. B **54**, 1703 (1996).
[71] S. H. Vosko, L. Wilk, and M. Nusair, Can. J. Phys. **58**, 1200 (1980).
[72] D. M. Ceperley and B. J. Alder, Phys. Rev. Lett. **45**, 566 (1980).
[73] L. Hedin and B. I. Lundqvist, J. Phys. C **4**, 2064 (1971).
[74] Y. Wang and J. P. Perdew, Phys. Rev. B **44**, 13298 (1991).
[75] W. R. L. Lambrecht, S. Limpijumnong, and B. Segall, MRS Internet J. Nitride Semicond. Res. **4S1**, G6.8 (1999).
[76] R. Ahuja, L. Fast, O. Eriksson, J. M. Wills, and B. Johansson, J. Appl. Phys. **83**, 8065 (1998).
[77] H. Karzel, W. Potzel, M. Köfferlein, W. Schissl, M. Steiner, U. Hiller, G. M. Kalvius, D. W. Mitchell, T. P. Das, P. Blaha, K. Schwarz, and M. P. Pasternak, Phys. Rev. B **53**, 11425 (1996).
[78] A. E. Mattsson, R. Armiento, J. Paier, G. Kresse, J. M. Wills, and T. R. Mattsson, J. Chem. Phys. **128**, 084714 (2008).
[79] P. Haas, F. Tran, and P. Blaha, Phys. Rev. B **79**, 085104 (2009).
[80] R. W. G. Wyckoff, *Crystal Structures*, 2nd ed. (Interscience, New York, 1963), Vol. 1.
[81] M. J. L. Sangster and A. Stoneham, Philos. Mag. B **43**, 597 (1981).
[82] A. J. Cohen and R. G. Gordon, Phys. Rev. B **14**, 4593 (1976).
[83] M. J. L. Sangster, G. Peckham, and D. H. Saunderson, J. Phys. C **3**, 1026 (1970).
[84] N. Y. Moghadam, G. M. Stocks, X.-G. Zhang, D. M. C. Nicholson, W. A. Shelton, Y. Wang, and J. S. Faulkner, J. Phys.: Condens. Matter **13**, 3073 (2001).
[85] L. Hedin and S. Lundqvist, in *Solid State Physics*, edited by F. Seitz and D. Turnbull (Academic, New York, 1969), Vol. 23.
[86] L. J. Sham and M. Schlüter, Phys. Rev. B **32**, 3883 (1985).
[87] R. W. Godby, M. Schlüter, and L. J. Sham, Phys. Rev. Lett. **56**, 2415 (1986).
[88] S. Kümmel and L. Kronik, Rev. Mod. Phys. **80**, 3 (2008).
[89] U. Schönberger and F. Aryasetiawan, Phys. Rev. B **52**, 8788 (1995).
[90] R. A. Powell, W. E. Spicer, and J. C. McMenamin, Phys. Rev. Lett. **27**, 97 (1971).
[91] C. J. Vesely, R. L. Hengehold, and D. W. Langer, Phys. Rev. B **5**, 2296 (1972).
[92] J. C. Slater, Adv. Quantum Chem. **6**, 1 (1972).
[93] D. A. Liberman, Phys. Rev. B **62**, 6851 (2000).
[94] J. G. Harrison, R. A. Heaton, and C. C. Lin, J. Phys. B **16**, 2079 (1983).